Prazosin-Related Compounds. Effect of Transforming the Piperazinylquinazoline Moiety into an Aminomethyltetrahydroacridine System on the Affinity for α_1-Adrenoreceptors

Michela Rosini,[†] Alessandra Antonello,[†] Andrea Cavalli,[†] Maria L. Bolognesi,[†] Anna Minarini,[†] Gabriella Marucci,[‡] Elena Poggesi,[§] Amedeo Leonardi,[§] and Carlo Melchiorre*[,†]

Department of Pharmaceutical Sciences, University of Bologna, Via Belmeloro 6, 40126 Bologna, Italy, Department of Chemical Sciences, University of Camerino, Via S. Agostino 1, 62032 Camerino (MC), Italy, and Research and Development Division, Recordati S.p.A., Via Civitali 1, 20148 Milano, Italy

Received July 8, 2003

In a search for structurally new α_1-adrenoreceptor (α_1-AR) antagonists, prazosin (**1**)-related compounds **2**−**11** were synthesized and their affinity profiles were assessed by functional experiments in isolated rat vas deferens (α_{1A}), spleen (α_{1B}), and aorta (α_{1D}) and by binding assays in CHO cells expressing human cloned α_1-AR subtypes. Transformation of the piperazinylquinazoline moiety of **1** into an aminomethyltetrahydroacridine system afforded compound **2**, endowed with reduced affinity, in particular for the α_{1A}-AR subtype. Then, to investigate the optimal features of the tricyclic moiety, the aliphatic ring of **2** was modified by synthesizing the lower and higher homologues **3** and **4**. An analysis of the pharmacological profile, together with a molecular modeling study, indicated the tetrahydroacridine moiety as the most promising skeleton for α_1-antagonism. Compounds **5**−**8**, where the replacement of the furoyl group of **2** with a benzoyl moiety afforded the possibility to evaluate the effect of the substituent trifluoromethyl on receptor binding, resulted, except for **7**, in a rather surprising selectivity toward α_{1B}-AR, in particular vs the α_{1A} subtype. Also the insertion of the 2,6-dimethoxyphenoxyethyl function of WB 4101 on the tetrahydroacridine skeleton of **2**, and/or the replacement of the aromatic amino function with a hydroxy group, affording derivatives **9**−**11**, resulted in α_{1B}-AR selectivity also vs the α_{1D} subtype. On the basis of these results, the tetrahydroacridine moiety emerged as a promising tool for the characterization of the α_1-AR, owing to the receptor subtype selectivity achieved by an appropriate modification of the lateral substituents.

Introduction

In recent years, the heterogeneity of the α_1-adrenoreceptors (α_1-ARs) has been claimed both on a molecular and pharmacological level. The latest picture of α_1-ARs shows at least three well-characterized subtypes, namely, α_{1A} (α_{1a}), α_{1B} (α_{1b}), and α_{1D} (α_{1d}), with upper and lower case subscripts being used to designate native or recombinant receptor, respectively,[1,2] while evidence with regard to a putative α_{1L}-AR now suggests it is a functional phenotype of the α_{1A}-AR.[3]

The effort to design agents selective for each of the three α_1-AR subtypes has been an active area of research. Whereas the efficacy of α_{1A}-AR antagonists in the treatment of benign prostatic hyperplasia has been demonstrated[4,5] and the role of the α_{1B}-AR subtype in the regulation of blood pressure has recently been advanced,[6] a potential therapeutic use for the α_{1D}-AR subtype has not been firmly established yet.

In continued efforts to identify high-affinity, selective ligands for subtypes of the α_1-AR, our research group has long being involved in designing new α_1-AR antagonists structurally related to prazosin (**1**),[7−13] the prototype of quinazoline-bearing compounds widely used as a pharmacological tool for α_1-AR subtypes characterization and as an effective drug in the management of hypertension. In previous studies both the piperazine moiety and the furan ring of prototype **1** have been modified, affording antagonists that are able to differentiate among α_1-AR subtypes.[11] This observation may form the basis to further modify the structure of these analogues, in an attempt to improve the selectivity.

In 1987, Campbell and co-workers,[14] in order to rationalize the exceptional α_1-AR affinity and α_1-competitive antagonism displayed by certain 2,4-diamino-6,7-dimethoxyquinazoline derivatives, visualized these compounds as conformationally restricted analogues of noradrenaline. Following X-ray analyses and molecular mechanics calculations, they could advance that a dominant role in the receptor recognition process was played by the protonated N_1 of the quinazoline system, which should mime the amine function of the neurotransmitter, protonated at physiological pH. In particular, they pointed out a charged-reinforced H-bond interaction involving the quinazoline-N_1 function and an anionic site of the receptor. The relevance of the N_1-protonation in receptor binding was also confirmed through the synthesis of a series of quinoline-analogues of **1**, in which the removal of the N_3 function resulted in an increased α_1-AR affinity, accordingly with a

* Corresponding author. Tel. +39-051-2099706. Fax: +39-051-2099734. E-mail: camelch@kaiser.alma.unibo.it.
[†] University of Bologna.
[‡] University of Camerino.
[§] Recordati S.p.A.

10.1021/jm030952q CCC: $25.00
Published on Web 10/10/2003

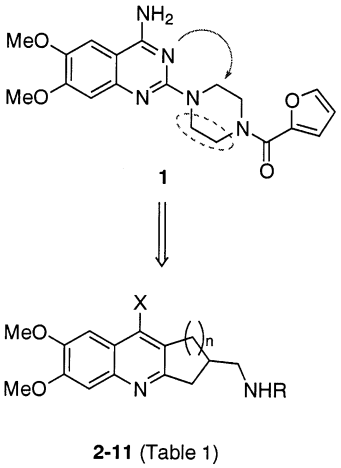

Figure 1. Design strategy for the synthesis of **2**−**11** by connecting the piperazine ring of **1** to a quinoline ring system.

significantly enhanced basicity of the N_1 nitrogen, with respect to the prototype.[15] Moreover, the role of the N_1 function in the receptor recognition process was also assessed through a series of isoquinoline derivatives in which the lack of this nitrogen atom resulted in no significant affinity for α_1-AR.[16]

Very recently, a further interaction model **1**-α_1-ARs suggested the N_1 function on the quinazoline ring to be one of the key groups involved in receptor binding, together with the two methoxy moieties, the 4-amino group, and the carbonyl function. Docking studies revealed that the N_1 moiety should possibly interact, by hydrogen-bond formation, with the hydroxyl group of a serine residue of TM5, which is present in all of the three subtypes. Moreover, an identical number of binding sites for **1** within all the α_1-AR subtypes was advanced, **1** supposedly interacting with amino acids in the same positions and in identical helices of α_{1A}, α_{1B}, and α_{1D} receptors, thus accounting for the nonselectivity of this ligand within α_1-ARs.[17]

With the aim of improving the selectivity profile at α_1-AR, in this study **1** was further modified, affording a series of derivatives in which the N_1 function is preserved, even if included in a different cyclic system. Actually, since the synthesis of constrained analogues of a lead compound represents a useful approach when searching for clues about binding site topography, we modified the quinazoline system into a tetrahydroacridine ring, affording **2** (Figure 1). This structural modification, in addition to preserving N_1 basicity, could force N_1 and the furan moiety to assume a reciprocal arrangement likely similar to that of prazosin in one of its low-energy conformations. Moreover, since the N_3 function is not essential for α_1-AR affinity, we thought that its removal should not negatively affect the activity of these tetrahydroacridine derivatives at α_1-ARs.

To test such a hypothesis, a molecular modeling study was carried out. In particular, the three-dimensional model of our target molecule, **2**, was built and analyzed by means of a Monte Carlo conformational search. Then, this was superimposed onto the crystallographic 3D structure of **1**, as retrieved from the Cambridge Structural Databank. The quite good superimposition obtained between **2** and **1** (Figure 2) prompted us to carry out the synthesis of the present series of derivatives.

To evaluate the effect of a different relative position of N_1 function and furan moiety on α_1-AR affinity and selectivity, analogues **3** and **4**, where a cyclopentane and a cycloheptane moiety replaced the cyclohexane ring, respectively, were synthesized.

The presence of a phenyl in place of the furan ring of **1** in related analogues had previously afforded the opportunity to examine the effect of substituents on both potency and selectivity toward α_1-AR subtypes, through the insertion, in all positions of the phenyl ring, of properly chosen groups.[13] Since the unsubstitued analogue, together with compounds with the trifluoromethyl group in the ortho, meta, or para position, resulted in the most intriguing molecules because of their α_{1D} selectivity, the same structural modifications were performed on **2**, providing tetrahydroacridine analogues **5**−**8**.

Moreover, because the 2,6-dimethoxyphenoxyethyl function of WB 4101 {*N*-[2-(2,6-dimethoxyphenoxy)-ethyl]-2,3-dihydro-1,4-benzodioxin-2-methanamine}, the prototype of benzodioxan-bearing compounds as α_1-AR selective antagonist, is a key pharmacophore at this receptor type,[18] we thought it of interest to combine, in the same molecule, this moiety and the tetrahydroacridine system of **2**, affording the hybrid structure **9**.

Finally, we synthesized compounds **10** and **11**, where the 4-amino group of **2** and **9**, respectively, was replaced with a hydroxyl moiety, with the aim of verifying if this structural modification could differently affect affinity for α_1-AR subtypes.

We describe here the synthesis and the pharmacological profile of tetrahydroacridines **2**−**11** in functional and binding experiments in comparison with prototypes prazosin (**1**) and WB 4101.

Chemistry

All the compounds were synthesized by standard procedures (Schemes 1−3) and were characterized by IR, ^{1}H NMR, mass spectra, and elemental analysis. The structure of key intermediates **12**−**14** and of isomers **18** and **19** was assigned by means of ^{1}H NMR and COSY experiments.

The synthesis of compounds **2**−**4** was achieved by condensation of 2-amino-4,5-dimethoxybenzonitrile with the appropriate cycloketone in the presence of $ZnCl_2$, followed by reduction of the nitro group of derivatives **12**−**14** and coupling of the obtained amines (**15**−**17**) with 2-furoyl chloride. 3-(Nitromethyl)cyclopentanone, 3-(nitromethyl)cyclohexanone, and 3-nitromethylcycloheptanone were synthesized using, as starting materials, nitromethane and the appropriate α,β-unsaturated cycloketone according to Rosini et al.[19] Similarly, compounds **5**−**8** were obtained through amidation of **15** with benzoyl chloride or with the appropriate (trifluoromethyl)benzoyl chloride, which was generated in situ by treating the corresponding (trifluoromethyl)benzoic acid with $SOCl_2$ (Scheme 1).

Condensation of **15** with 2-(2,6-dimethoxyphenoxy)-acetaldehyde,[20] followed by reduction of the intermediate Schiff base with $NaBH_4$, afforded the hybrid structure **9**, as depicted in Scheme 2.

Finally, the $POCl_3$-mediated condensation between 4,5-dimethoxyanthranilic acid and 3-(nitromethyl)cyclohexanone afforded the two possible structural isomers

Scheme 1

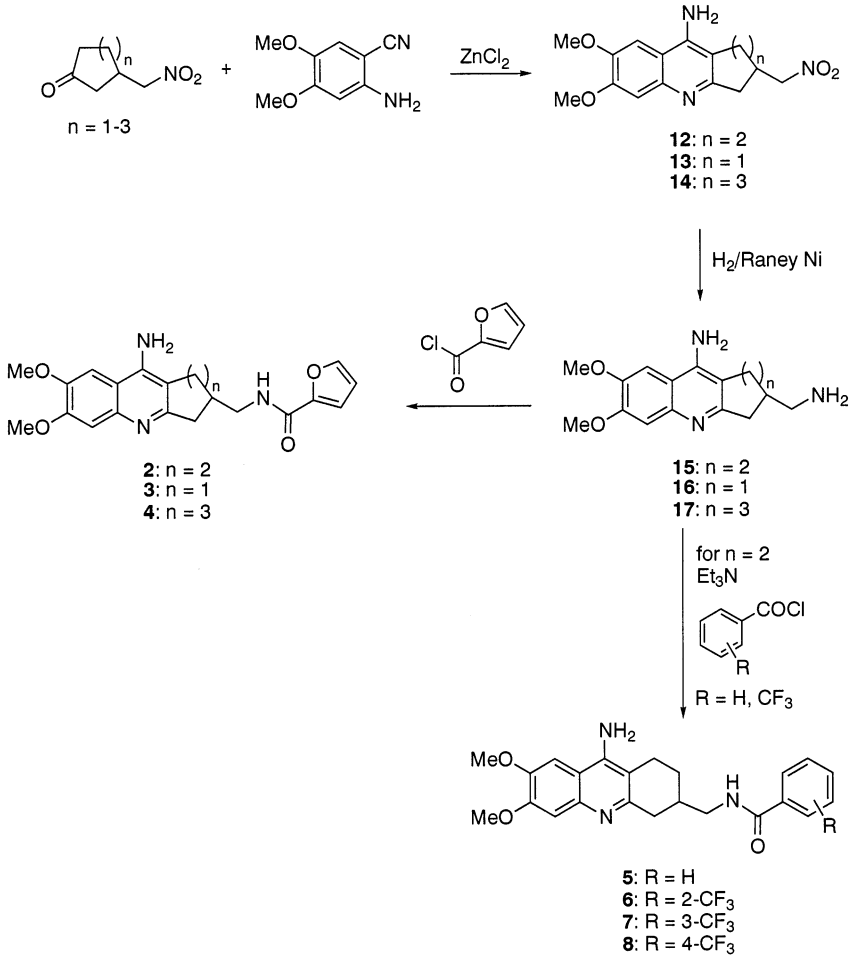

Scheme 2

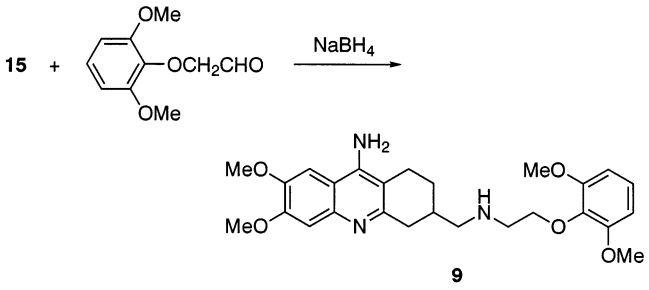

18 and **19**. Reduction of the nitro function of **19** with Raney Ni afforded the corresponding amine **20**, which, in turn, was submitted to coupling reaction with 2-furoyl chloride, providing **10**, or condensed with 2-(2,6-dimethoxyphenoxy)acetaldehyde,[20] to give **11** (Scheme 3).

Biology

Functional Studies. Receptor subtype selectivity of compounds **2**−**11** was determined at α_1-ARs on different isolated rat tissues using **1** and WB 4101 as reference standards. α_1-AR subtypes blocking activity was assessed by antagonism of (−)-noradrenaline-induced contraction of prostatic vas deferens (α_{1A})[21] or thoracic aorta (α_{1D})[22] and by antagonism of (−)-phenylephrine-induced contraction of rat spleen (α_{1B}).[23] Furthermore, compounds **2** and **9**, owing to their structural analogy with tacrine, were evaluated also for their inhibitory activity of AChE from human serum.

Binding Experiments. The pharmacological profile of compounds **2**, **3**, and **6**−**11** was further evaluated by radioreceptor binding assays using **1** and WB 4101 as reference standards. [^{3}H]Prazosin was used to label cloned human α_1-ARs expressed in Chinese hamster ovary (CHO) cells.[24]

Results and Discussion

The affinity for the three α_1-AR subtypes of compounds used in the present study was expressed as pK_b and pK_i values and values are shown in Table 1. To make relevant considerations on structure−activity relationships, prototype **1** and WB 4101 were included for comparison. All the tetrahydroacridine derivatives behaved, like **1**, as competitive antagonists, as they did not affect the maximal responses induced by the agonist while causing a parallel shift to the right of the concentration−response curves to the agonist. Although compounds **2** and **9** bear in their structure the tetrahydroacridine moiety of tacrine, a well-known AChE inhibitor, they were poor AChE inhibitors as revealed by their pIC_{50} values of 5.30 ± 0.11 and 5.05 ± 0.07, respectively.

Since the affinities of all of the novel analogues at α_1-adrenoreceptor subtypes were substantially lower than the prototype **1**, the enantiomers produced by the introduction of the chiral center were not separated. In molecular modeling studies to establish the putative active enantiomer, either *R* or *S* of **3** was superimposed onto the template, i.e., the energy-minimized crystal

Scheme 3

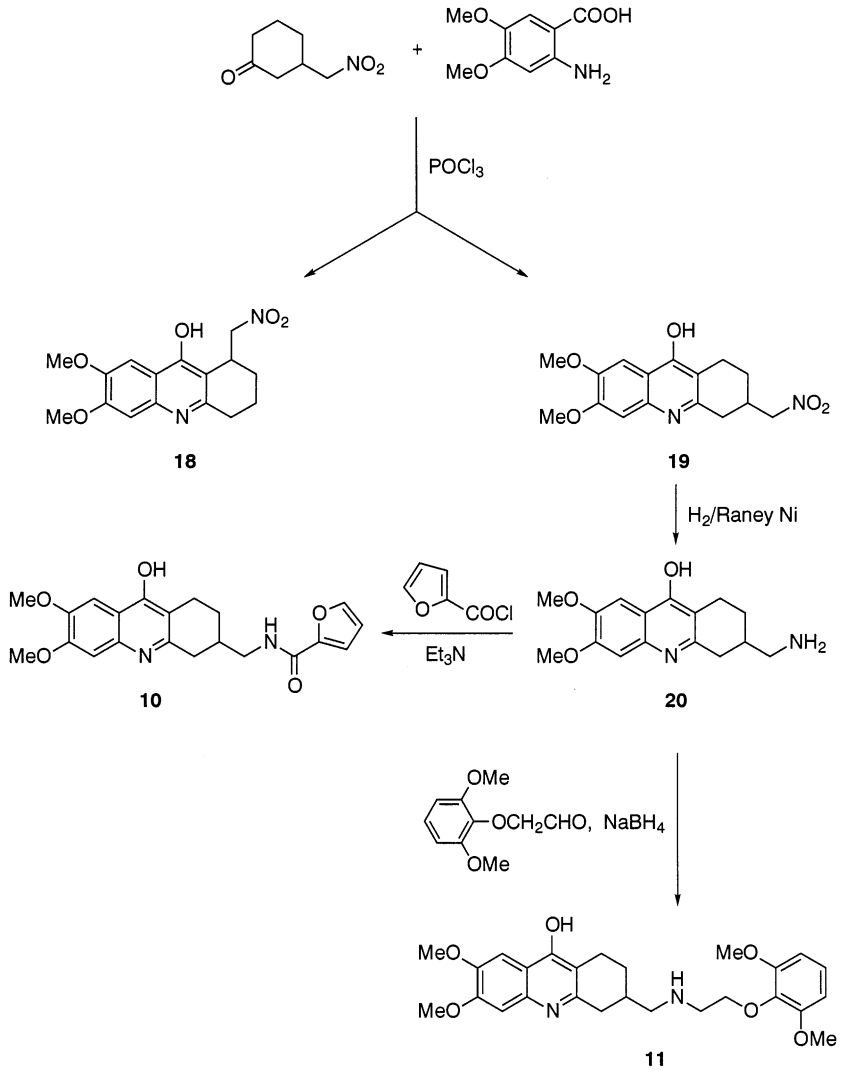

Table 1. Affinity Constants, Expressed as pK_B (Isolated Tissues) or pK_i (CHO Cells) Values, of **1**−**11** and WB4101 at α_1-ARs on Isolated Prostatic Vas Deferens (α_{1A}), Spleen (α_{1B}), and Thoracic Aorta (α_{1D}) and at Human Recombinant α_1-AR Subtypes (pK_i)

	pK_B[a]			pK_i[b]		
compd	α_{1A}	α_{1B}	α_{1D}	α_{1a}	α_{1b}	α_{1d}
1	8.93 ± 0.09	9.06 ± 0.11	8.93 ± 0.10	9.23	9.39	9.65
2	6.52 ± 0.05	7.30 ± 0.20	7.47 ± 0.16	7.02	7.91	7.80
3	6.26 ± 0.08	6.82 ± 0.04	6.11 ± 0.12	6.80	7.10	6.70
4	6.34 ± 0.21	6.92 ± 0.11	6.94 ± 0.08			
5	6.67 ± 0.22	7.19 ± 0.08	6.63 ± 0.18			
6	6.47 ± 0.14	7.33 ± 0.25	6.85 ± 0.08	6.54	8.13	7.61
7	7.16 ± 0.08	7.36 ± 0.03	7.58 ± 0.23	7.50	7.90	7.60
8	6.08 ± 0.08	7.20 ± 0.14	6.67 ± 0.11	7.07	8.05	7.72
9	5.70 ± 0.11	7.20 ± 0.11	6.39 ± 0.09	6.01	7.40	6.70
10	5.76 ± 0.08	6.95 ± 0.09	6.41 ± 0.07	5.59	6.53	5.94
11	6.24 ± 0.13	7.05 ± 0.09	5.92 ± 0.05	5.77	6.66	6.41
WB4101	9.48 ± 0.09	8.20 ± 0.11	8.85 ± 0.12	9.37	8.0	9.29

[a] pK_B values ± SE were calculated at one concentration (in the range of 0.1−10 μM) according to van Rossum.[31] Each concentration was tested from four to five times. [b] Equilibrium dissociation constants (K_i) were derived from IC_{50} values using the Cheng−Prusoff equation.[33] Each experiment was performed in triplicate. K_i values were from two or three experiments, which agreed within ±20%.

structure of **1**. Actually, **3** is the less flexible antagonist of the present series, being the tricyclic system coplanar. Therefore, for each enantiomer of **3** only one conformation for the tricyclic moiety was detected. It turned out that the *S*-enantiomer fitted onto **1** better than the *R*-enantiomer (RMSD equal to 0.945 and 1.706 Å, respectively). Therefore, in the following, only *S*-enantiomers of the present series of derivatives were taken into account, since they were considered to be those biologically active.

Once established that the likely active enantiomer of this series of antagonists was the *S* one, we focused on the lead compound of the present series, **2**, synthesized in an attempt to identify a new lead as α_1-AR antagonist, based on a tetrahydroacridine skeleton. The tricyclic moiety of the *S*-enantiomer of **2** provided two different conformations, being the substituent in position 3 of the tricyclic moiety either axial or equatorial. The heats of formation of the two conformers showed that the equatorial was more stable than the axial one by almost 2 kcal/mol. More interestingly, the best fitting equatorial conformer superimposed much better onto **1** than the best fitting axial one (RMSD = 0.769 and 1.988 Å, respectively). This showed that the equatorial conformer was most likely to be the active one.

The intriguing similarity shown by **1** and **2**, with respect to the relative positions of the pharmacophoric functions, suggested that **2** should possibly fit with the same amino acids of the α_1-AR involved in prazosin

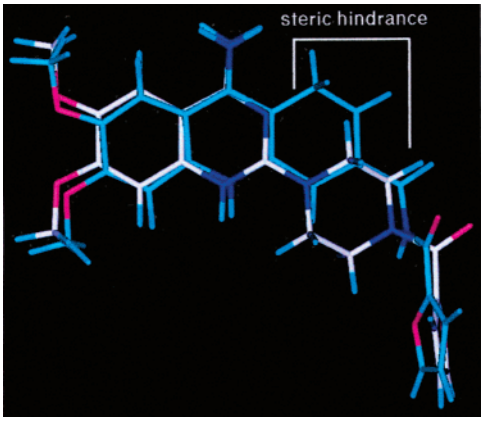

Figure 2. Superimposition of AM1-minimized low-energy conformation of **2** (carbon atoms are green) onto the AM1-minimized **1** crystal structure. The superimposition was accomplished by fitting the following atoms: the oxygen atoms of the methoxy groups, the pyridine and the aniline nitrogen atoms, the carbonyl oxygen, a carbon and the oxygen atoms of the furan ring. The pharmacophoric functions of **2** fit well those of **1**. However, the steric hindrance of the aliphatic portion of **2** could prevent optimal interactions with the biological counterpart.

binding. Notwithstanding, the affinity profile of **2** at α_1-ARs resulted to be significantly different from that displayed by the prototype. Actually, **2** was found to be more than 2 orders of magnitude weaker at the α_{1A}-AR subtype and between one and 2 orders of magnitude less potent at α_{1B}- and α_{1D}-AR subtypes in functional assays. A similar trend was observed in binding experiments. Although **2** appears to be capable of all of the key antagonist-receptor interactions shown for **1** in the models previously described, a 3D model of the superimposition showed that the loss of potency could be ascribed to the steric hindrance induced by the newly introduced aliphatic portion of the tetrahydroacridine backbone of **2** (Figure 2). To verify such a hypothesis, the aliphatic ring of **2** was modified by synthesizing its lower and higher homologues, **3** and **4**, respectively. Both of these compounds were identified to be slightly less potent than **2** at all the α_1-AR subtypes, except for the affinity of **3** at the α_{1D} subtype, which was significantly reduced. The worse capability of derivatives **3** and **4** to fit **1** (**3**, RMSD of 0.945 Å; **4**, RMSD of 1.306 Å) could be mainly responsible for this loss of affinity, thus not allowing an appropriate evaluation of the effect of steric hindrance in receptor binding. However, the higher α_{1D} affinity of **4** versus **3** cannot be easily explained by the present biological data and molecular modeling results.

The tetrahydroacridine moiety of **2** proved to be the most promising skeleton for α_1-AR antagonism and, consequently, its structure was further modified in order to explore affinity and selectivity toward α_1-AR subtypes.

The efficacy of the trifluoromethyl substituent on the phenyl ring of prazosin analogues in inducing selectivity toward the α_{1D}-AR subtype has previously been reported.[13] The same structural modifications, performed on **2**, provided analogues **5**−**8**. With the exception of **7**, rather surprisingly, these compounds displayed an appreciable selectivity for the α_{1B}-AR subtype. It is evident that the replacement of the quinazoline system with a tetrahydroacridine ring negatively affects affinity for α_{1A}- and α_{1D}-ARs, thus inducing relative α_{1B}-AR subtype selectivity. For all the derivatives of this series, the major negative effect of the tetrahydroacridine skeleton is observed for the α_{1D}-AR subtype, which looks more sensitive to the steric hindrance enhancement produced by this moiety relative to the quinazoline system of **1**.

The inclusion of the 2,6-dimethoxyphenoxyethyl function of the potent and selective α_{1A}-AR antagonist WB 4101 onto the tetrahydroacridine skeleton of **2**, giving compound **9**, led to a very different affinity profile at the α_{1A}-AR subtype with respect to prototypes: the α_{1A} pK_B value for **9** was 4575-fold lower than that for WB 4101 and 7-fold lower than that for **2**. An analysis of the structural features of the tetrahydroacridine skeleton of **2** and of the benzodioxan moiety of WB 4101 clearly reveals key physicochemical differences. As a matter of fact, in this contest, the presence, in **9**, of a second basic function, may assume a relevant role in determining a different ligand−receptor recognition process. Interestingly, however, **9** turned out to be as potent as **2** at the α_{1B}-AR, suggesting that the lateral substituent inserted onto the tetrahydroacridine skeleton is not able to effectively tune affinity at this site.

The behavior at the α_{1D}-AR subtype is intermediate between α_{1A}- and α_{1B}-AR subtypes.

Replacement of the amino function of **9** with a hydroxy group, affording compound **11**, resulted in a 35-fold higher affinity at α_{1A}-AR in functional experiments. The finding that the same modification, performed on **2** to give **10**, resulted instead in a decreased potency at the α_{1A}-AR subtype, put in evidence the importance of the lateral chain in determining affinity for this receptor type.

In conclusion, the modification of the piperazinylquinazoline moiety of **1** into an aminomethyltetrahydroacridine system afforded compounds **2**−**11**. The whole series of derivatives resulted to be less potent at all α_1-AR subtypes relative to prototype **1**, most of them displaying a tendency to selectivity for the α_{1B}-AR subtype both in functional and binding experiments. The newly introduced tricyclic system represents an interesting pharmacophore at the α_{1B}-AR subtype, leading to a significant affinity, which does not seem to be greatly influenced by the lateral substituent. On the contrary, the pharmacological profile of these compounds at α_{1A}- and α_{1D}-ARs is significantly influenced by the nature of the lateral chain, thus providing the opportunity to modulate selectivity for the α_{1B}-AR by means of an appropriate modification of their structure.

Experimental Section

Chemistry. Melting points were taken in glass capillary tubes on a Büchi SMP-20 apparatus and are uncorrected. IR, electron impact (EI) mass, and direct infusion ESI-MS spectra were recorded on Perkin-Elmer 297, VG 7070E, and Waters ZQ 4000 apparatus, respectively. ^{1}H NMR and COSY experiments were recorded on Mercury 400 and Varian VXR 300 instruments. Chemical shifts are reported in parts per million (ppm) relative to tetramethylsilane (TMS), and spin multiplicities are given as s (singlet), br s (broad singlet), d (doublet), t (triplet), or m (multiplet). Although the IR spectra data are not included (because of the lack of unusual features), they were obtained for all compounds reported and were consistent with the assigned structures. The elemental compositions of the compounds agreed to within ±0.4% of the calculated value.

When the elemental analysis is not included, crude compounds were used in the next step without further purification. Chromatographic separations were performed on silica gel columns by flash (Kieselgel 40, 0.040−0.063 mm; Merck) or gravity column (Kieselgel 60, 0.063−0.200 mm; Merck) chromatography. Compounds were named following IUPAC rules as applied by Beilstein-Institut AutoNom (version 2.1), a PC integrated software package for systematic names in organic chemistry.

6,7-Dimethoxy-3-(nitromethyl)-1,2,3,4-tetrahydroacridin-9-ylamine (12). A mixture of 2-amino-4,5-dimethoxybenzonitrile (1.0 g, 5.61 mmol), 3-(nitromethyl)cyclohexanone[19] (0.88 g, 5.61 mmol), and dry $ZnCl_2$ (1.7 g) was heated at 100 °C for 3 h. After cooling, the reaction mixture was treated with 1 N NaOH and the separated solid, collected by filtration, was washed with ether (2 × 30 mL), $CHCl_3$ (2 × 30 mL), and EtOAc (2 × 30 mL), affording crude **12**: 40% yield; ^{1}H NMR (DMSO-d_6) δ 1.55−1.62 (m, 1), 1.92−2.02 (m, 1), 2.45−2.76 (m, 4), 2.82−2.91 (m, 1), 3.78 (s, 3), 3.81 (s, 3), 4.61 (d, 2), 6.20 (br s, exchangeable with D_2O, 2), 7.02 (s, 1), 7.40 (s, 1); EI MS *m*/*z* 317 (M^+).

6,7-Dimethoxy-2-(nitromethyl)-2,3-dihydro-1*H*-cyclopenta[*b*]quinolin-9-ylamine (13) was synthesized from 2-amino-4,5-dimethoxybenzonitrile (1.88 g, 10.55 mmol) and 3-(nitromethyl)cyclopentanone[19] (1.51 g, 10.55 mmol) by following the procedure described for **12**, affording crude **13**: 35% yield; ^{1}H NMR (DMSO-d_6) δ 2.58−2.79 (m, 2), 2.99−3.21 (m, 3), 3.90 (s, 3), 3.92 (s, 3), 4.60−4.82 (m, 2), 6.35 (br s, exchangeable with D_2O, 2); 7.10 (s, 1), 7.45 (s, 1).

2,3-Dimethoxy-7-(nitromethyl)-7,8,9,10-tetrahydro-6*H*-cyclohepta[*b*]quinolin-11-ylamine (14) was synthesized from 2-amino-4,5-dimethoxybenzonitrile (2.08 g, 11.67 mmol) and 3-(nitromethyl)cycloheptanone[19] (2 g, 11.67 mmol) by following the procedure described for **12**, affording crude **14**: 47% yield; ^{1}H NMR (DMSO-d_6) δ 1.16−1.62 (m, 2), 1.78−1.98 (m, 2), 2.15−2.36 (m, 1), 2.42−2.61 (m, 1), 2.79−3.10 (m, 3), 3.82 (s, 3), 3.86 (s, 3), 4.45 (t, 2), 6.21 (br s, exchangeable with D_2O, 2), 7.05 (s, 1), 7.42 (s, 1).

3-(Aminomethyl)-6,7-dimethoxy-1,2,3,4-tetrahydroacridin-9-ylamine (15). A suspension of **12** (0.18 g, 0.57 mmol) and Raney Ni (nickel sponge; suspension in water) (0.10 g) in MeOH (20 mL) and CH_3COOH (5 mL) was hydrogenated for 6 h at room temperature. Following catalyst removal, the solvent was evaporated, yielding a residue that was dissolved in water, treated with 40% NaOH, and continuously extracted with $CHCl_3$ (50 mL). Removal of the dried solvent gave a residue that was purified by flash chromatography. Elution with $CHCl_3$/MeOH/aqueous 30% ammonia (6:4:0.4) afforded **15** as a yellow solid: 75% yield; mp 144−148 °C; ^{1}H NMR (DMSO-d_6) δ 1.23−1.42 (m, 1), 1.61−1.75 (m, 1), 2.01−2.18 (m, 1), 2.33−2.78 (m, 5), 2.80−2.96 (m, 1), 3.83 (s, 3), 3.86 (s, 3), 6.15 (br s, exchangeable with D_2O, 2), 7.02 (s, 1), 7.42 (s, 1).

2-(Aminomethyl)-6,7-dimethoxy-2,3-dihydro-1*H*-cyclopenta[*b*]quinolin-9-ylamine (16) was synthesized from **13** (0.31 g, 1.02 mmol) by following the procedure described for **15** and purified by flash chromatography. Elution with a step gradient system of $CHCl_3$/MeOH/aqueous 30% ammonia (9:1:0.1 to 8.5:1.5:0.15) afforded **16** as a white solid: 90% yield; mp 148−150 °C; ^{1}H NMR (CD_3OD) δ 2.61−2.70 (m, 1), 2.72−2.85 (m, 2), 2.97 (d, 2), 3.05−3.29 (m, 2), 3.98 (s, 3), 4.02 (s, 3), 7.18 (s, 1), 7.45 (s, 1); MS (ESI^+) *m*/*z* 274 $(M + H)^+$.

7-(Aminomethyl)-2,3-dimethoxy-7,8,9,10-tetrahydro-6*H*-cyclohepta[*b*]quinolin-11-ylamine (17) was synthesized from **14** (0.35 g, 1.16 mmol) by following the procedure described for **15** and purified by flash chromatography. Elution with $CHCl_3$/MeOH/aqueous 30% ammonia (8.5:1.5:0.15) afforded **17** as a white solid: 87% yield; mp 138−140 °C; ^{1}H NMR (CD_3OD) δ 1.20−1.55 (m, 3), 1.75−2.03 (m, 2), 2.35−2.58 (m, 3), 2.65−2.90 (m, 3), 3.90 (s, 3), 3.92 (s, 3), 7.05 (s, 1), 7.23 (s, 1).

Furan-2-carboxylic Acid (9-Amino-6,7-dimethoxy-1,2,3,4-tetrahydroacridin-3-ylmethyl)amide hydrochloride (2). A solution of 2-furoyl chloride (0.034 mL, 0.35 mmol) in dry EtOH (2 mL) was added dropwise to a solution of **15** (0.10 g, 0.35 mmol) and triethylamine (0.048 mL, 0.35 mmol) in dry EtOH (10 mL). Stirring at room temperature for 24 h afforded **2** as a white solid that was collected by filtration and transformed into the hydrochloride salt: 80% yield; mp 220−222 °C (from EtOH); ^{1}H NMR (CD_3OD) δ 1.60−1.78 (m, 1), 2.18−2.25 (m, 2), 2.51−2.82 (m, 3), 3.01−3.16 (m, 1), 3.46 (t, 2), 3.99 (s, 3), 4.01 (s, 3), 6.60−6.65 (m, 1), 7.03 (s, 1), 7.18 (d, 1), 7.61 (s, 1), 7.68−7.71 (m, 1); EI MS *m*/*z* 381 (M^+). Anal. ($C_{21}H_{24}ClN_3O_4$) C, H, N.

Furan-2-carboxylic acid (9-amino-6,7-dimethoxy-2,3-dihydro-1*H*-cyclopenta[*b*]quinolin-2-ylmethyl)amide hydrochloride (3) was synthesized from **16** (0.10 g, 0.37 mmol), triethylamine (0.051 mL, 0.37 mmol), and 2-furoyl chloride (0.036 mL, 0.37 mmol) by following the procedure described for **2** and purified by flash chromatography. Elution with $CHCl_3$/MeOH/aqueous 30% ammonia (9:1:0.06) afforded crude **3** that was transformed into the hydrochloride salt: 65% yield; mp 263−265 °C (from ether/EtOH); ^{1}H NMR (CD_3OD) δ 2.12−2.19 (m, 1), 2.25−3.15 (m, 4), 3.48 (t, 2), 3.86 (s, 3), 3.91 (s, 3), 6.58−6.60 (m, 1), 7.02 (s, 1), 7.14 (d, 1), 7.28 (s, 1), 7.68 (s, 1); MS (ESI^+) *m*/*z* 368 $(M+H)^+$. Anal. ($C_{20}H_{22}ClN_3O_4$) C, H, N.

Furan-2-carboxylic acid (11-amino-2,3-dimethoxy-7,8,9,10-tetrahydro-6*H*-cyclohepta[*b*]quinolin-7-ylmethyl)amide hydrochloride (4) was synthesized from **17** (0.10 g, 0.33 mmol), triethylamine (0.046 mL, 0.33 mmol), and 2-furoyl chloride (0.033 mL, 0.33 mmol) by following the procedure described for **2** and purified by flash chromatography. Elution with CH_2Cl_2/EtOH/aqueous 30% ammonia (8.5:1.5:0.01) afforded crude **4** that was transformed into the hydrochloride salt: 72% yield; mp 241−243 °C (from ether/EtOH); ^{1}H NMR (DMSO-d_6) δ 1.10−1.61 (m, 2), 1.78−1.97 (m, 3), 2.60−2.77 (m, 1), 3.04−3.22 (m, 5), 4.95 (s, 3), 4.97 (s, 3), 6.58−6.65 (m, 1), 7.18 (d, 1), 7.25 (s, 1), 7.81 (d, 2), 8.20 (br s, exchangeable with D_2O, 2), 8.58 (t, exchangeable with D_2O, 1); MS (ESI^+) *m*/*z* 396 $(M + H)^+$. Anal. ($C_{22}H_{26}ClN_3O_4$) C, H, N.

***N*-(9-Amino-6,7-dimethoxy-1,2,3,4-tetrahydroacridin-3-ylmethyl)benzamide hydrocloride (5)** was synthesized from **15** (0.045 g, 0.16 mmol), triethylamine (0.022 mL, 0.16 mmol), and benzoyl chloride (0.018 mL, 0.16 mmol) by following the procedure described for **2** and purified by flash chromatography. Elution with CH_2Cl_2/MeOH/aqueous 30% ammonia (9:1:0.1) afforded crude **5** that was transformed into the hydrochloride salt: 78% yield; mp 272−278 °C (from ether/EtOH);^{1}H NMR (CD_3OD) δ 1.40−1.58 (m, 1), 2.10−2.23 (m, 2), 2.42−2.78 (m, 3), 2.95−3.05 (m, 1), 3.43 (t, 2), 3.88 (s, 3), 3.92 (s, 3), 7.02 (s, 1), 7.30 (s, 1), 7.42−7.56 (m, 3), 7.86 (d, 2); MS (ESI^+) *m*/*z* 392 $(M + H)^+$. Anal. ($C_{23}H_{26}ClN_3O_3$) C, H, N.

***N*-(9-Amino-6,7-dimethoxy-1,2,3,4-tetrahydroacridin-3-ylmethyl)-2-(trifluoromethyl)benzamide hydrochloride (6).** A solution of 2-(trifluoromethyl)benzoic acid (0.033 g, 0.174 mmol) and $SOCl_2$ (0.13 mL, 1.74 mmol) in $CHCl_3$ was refluxed for 1 h. Removal of the solvent under reduced pressure afforded crude 2-(trifluoromethyl)benzoyl chloride in a quantitative yield. A solution of this chloride (0.036 g, 0.174 mmol) in dry $CHCl_3$ (2 mL) was added dropwise to a solution of **15** (0.050 g, 0.174 mmol) and triethylamine (0.036 mL, 0.260 mmol) in dry EtOH (8 mL). After the mixture was stirred at room temperature for 12 h, the solvent was removed under reduced pressure to give a residue that was purified by flash chromatography. Elution with $CHCl_3$/MeOH/aqueous 30% ammonia (9:1:0.04) afforded crude **6** that was transformed into the hydrochloride salt: 77% yield; mp 252−254 °C (from ether/EtOH); ^{1}H NMR (CD_3OD) δ 1.42−1.78 (m, 1H), 2.15−2.28 (m, 2H), 2.42−2.81 (m, 3H), 2.98−3.16 (m, 1H), 3.43 (d, 2H), 3.94 (s, 3H), 3.97 (s, 3H), 7,01 (s, 1H), 7.38 (s, 1H), 7.58−7.81 (m, 4H); MS (ESI^+) *m*/*z* 460 $(M + H)^+$. Anal. ($C_{24}H_{25}ClF_3N_3O_3$) C, H, N.

***N*-(9-Amino-6,7-dimethoxy-1,2,3,4-tetrahydroacridin-3-ylmethyl)-3-(trifluoromethyl)benzamide hydrochloride (7)** was synthesized from 3-(trifluoromethyl)benzoic acid (0.040 g, 0.209 mmol) and **15** (0.06 g, 0.209 mmol) by following the procedure described for **6** and purified by flash chroma-

tography. Elution with $CHCl_3$/MeOH/aqueous 30% ammonia (9:1:0.04) afforded crude **7** that was transformed into the hydrochloride salt: 65% yield; mp 250−252 °C (from ether/EtOH); ^{1}H NMR (CD_3OD) δ 1.46−1.70 (m, 1), 2.18−2.38 (m, 2), 2.57−2.84 (m, 3), 3.01−3.16 (m, 1), 3.52 (d, 2), 3.97 (s, 3), 4.01 (s, 3), 7.03 (s, 1), 7.40 (s, 1), 7.71 (t, 1), 7.84 (d, 1), 8.17−8.22 (m, 2); MS (ESI$^+$) *m/z* 460 $(M+H)^+$. Anal. ($C_{24}H_{25}ClF_3N_3O_3$) C, H, N.

***N*-(9-Amino-6,7-dimethoxy-1,2,3,4-tetrahydroacridin-3-ylmethyl)-4-(trifluoromethyl)benzamide hydrochloride (8)** was synthesized from 4-(trifluoromethyl)benzoic acid (0.033 g, 0.174 mmol) and **15** (0.05 g, 0.174 mmol) by following the procedure described for **6** and purified by flash chromatography. Elution with $CHCl_3$/MeOH/aqueous 30% ammonia (9:1:0.04) afforded crude **8** that was transformed into the hydrochloride salt: 70% yield; mp 253−255 °C (from ether/EtOH);^{1}H NMR (DMSO-d_6) δ 1.46−1.67 (m, 1), 2.08−2.28 (m, 2), 2.73−2.81 (m, 3), 3.03−3.16 (m, 1), 3.44 (t, 2), 3.96 (s, 3), 3.99 (s, 3), 7.22 (s, 1), 7.83 (s, 1), 7.92 (d, 2), 8.16 (d, 2), 9.01 (t, exchangeable with D_2O, 1); MS (ESI$^+$) *m/z* 460 $(M + H)^+$. Anal. ($C_{24}H_{25}ClF_3N_3O_3$) C, H, N.

3-{[2-(2,6-Dimethoxyphenoxy)ethylamino]methyl}-6,7-dimethoxy-1,2,3,4-tetrahydroacridin-9-ylamine dihydrochloride (9). A solution of 2-(2,6-dimethoxyphenoxy)acetaldehyde[20] (0.14, 0.70 mmol) in dry EtOH (2 mL) was added dropwise to a mixture of **15** (0.10 g, 0.35 mmol) and molecular sieves (3 Å) in dry MeOH (20 mL) over a period of 30 min at room temperature. $NaBH_4$ (0.030 g, 0.70 mmol) was then added and the stirring was continued for further 12 h. Following removal of molecular sieves, the solution was made acidic with 6 N HCl (1 mL). Removal of the solvent gave a residue, which was dissolved in water (10 mL). The solution was washed with ether (2 × 20 mL) to remove nonbasic materials and then was made basic with 2 N NaOH and finally extracted with $CHCl_3$ (3 × 20 mL). Removal of the dried solvent gave a residue that was purified by flash chromatography. Elution with $CHCl_3$/MeOH/aqueous 30% ammonia (9:1:0.05) afforded crude **9**, which was transformed into the hydrochloride salt: 65% yield; mp 247−253 °C (from ether/EtOH); ^{1}H NMR (CD_3OD) δ 1.42−1.58 (m, 1), 2.02−2.26 (m, 2), 2.53−2.79 (m, 5), 2.83 (t, 2), 2.98−3.06 (m, 1), 3.81 (s, 6), 3.91 (s, 3), 3.95 (s, 3), 4.09−4.15 (m, 2), 6.63 (d, 2), 7.01 (t, 1), 7.06 (s, 1), 7.37 (s, 1); MS (ESI$^+$) *m/z* 468 $(M + H)^+$. Anal. ($C_{26}H_{35}Cl_2N_3O_5$) C, H, N.

6,7-Dimethoxy-1-(nitromethyl)-1,2,3,4-tetrahydroacridin-9-ol (18) and 6,7-Dimethoxy-3-(nitromethyl)-1,2,3,4-tetrahydroacridin-9-ol (19). A mixture of 4,5-dimethoxyanthranilic acid (2.5 g, 12.72 mmol) and 3-(nitromethyl)cyclohexanone (2.0 g, 12.72 mmol) in $POCl_3$ (10 mL) was refluxed for 2 h. The reaction mixture was evaporated and treated with ice and solid $NaHCO_3$ until pH 7−8. The separated solid was taken up in ether, washed with water, dried, and evaporated to give a residue that was purified by flash chromatography. Elution with a step gradient system of CH_2Cl_2/EtOH/aqueous 30% ammonia (9.8:0.2:0.02 to 9:1:0.06) afforded **18** and **19**, respectively.

18: 35% yield; R_f 0.55 [$CHCl_3$/MeOH/aqueous 30% ammonia (9:1:0.04)]; mp 218−220 °C (from MeOH); ^{1}H NMR (DMSO-d_6) δ 1.82−1.93 (m, 4), 2.63 (t, 2), 3.58−3.75 (m, 1), 3.80 (s, 3), 3.82 (s, 3), 4.43 (t, 1), 4.83 (dd, 1), 6.84 (s, 1), 7.40 (s, 1), 11.40 (s, exchangeable with D_2O, 1); MS (ESI$^+$) *m/z* 319 $(M + H)^+$.

19: 30% yield; R_f 0.47 [$CHCl_3$/MeOH/aqueous 30% ammonia (9:1:0.04)]; mp 258−260 °C (from CH_2Cl_2); ^{1}H NMR (CD_3OD) δ 1.24−1.63 (m, 1), 2.02−2.18 (m, 1), 2.45−2.98 (complex m, 5), 3.88 (s, 3), 3.90 (s, 3), 4.58 (t, 2), 6.82 (s, 1), 7.61 (s, 1); MS (ESI$^+$) *m/z* 319 $(M + H)^+$.

3-(Aminomethyl)-6,7-dimethoxy-1,2,3,4-tetrahydroacridin-9-ol (20) was synthesized from **19** (0.22 g, 0.69 mmol) and Raney Ni (nickel sponge; suspension in water) (0.10 g) by following the procedure described for **15** and purified by flash chromatography. Elution with $CHCl_3$/MeOH/aqueous 30% ammonia (9:1:0.1) afforded **20** as a yellow solid: 77% yield; mp 245−250 °C; ^{1}H NMR (CD_3OD) δ 1.22−1.38 (m, 1), 1.72−1.84 (m, 1), 1.98−2.06 (m, 1), 2.30−2.46 (m, 2), 2.62−2.85 (m, 4), 3.82 (s, 3), 3.84 (s, 3), 6.63 (s, 1), 7.45 (s, 1).

Furan-2-carboxylic acid (9-hydroxy-6,7-dimethoxy-1,2,3,4-tetrahydroacridin-3-ylmethyl)-amide hydrochloride (10) was synthesized from **20** (0.40 g, 0.13 mmol), triethylamine (0.017 mL, 0.13 mmol), and 2-furoyl chloride (0.012 mL, 0.13 mmol) by following the procedure described for **2** and purified by flash chromatography. Elution with a step gradient system of CH_2Cl_2/EtOH (9.8:0.4 to 9:1) afforded crude **10** that was transformed into the hydrochloride salt: 76% yield; mp 205−209 °C (from ether/EtOH); ^{1}H NMR (CD_3OD) δ 1.60−1.78 (m, 1), 2.18−2.40 (m, 2), 2.70−3.26 (m, 4), 3.42−3.55 (m, 2), 4.02 (s, 3), 4.05 (s, 3), 6.59−6.63 (m, 1), 7.12−7.21 (m, 2), 7.67−7.72 (m, 2); MS (ESI$^+$) *m/z* 383 $(M + H)^+$. Anal. ($C_{21}H_{23}ClN_2O_5$) C, H, N.

3-{[2-(2,6-Dimethoxyphenoxy)ethylamino]methyl}-6,7-dimethoxy-1,2,3,4-tetrahydroacridin-9-ol dihydrochloride (11) was synthesized from **20** (0.15 g, 0.52 mmol), 2-(2,6-dimethoxyphenoxy)acetaldehyde[20] (0.20 g, 0.98 mmol), and $NaBH_4$ (0.37 g, 0.98 mmol) by following the procedure described for **9**. Removal of the solvent gave crude **11** that was transformed into the hydrochloride salt: 55% yield; mp 250−252 °C (from ether/EtOH); ^{1}H NMR ($CDCl_3$) δ 1.22−1.42 (m, 1), 1.92−2.18 (m, 2), 2.46−2.67 (m, 3), 2.80−3.10 (m, 5), 3.62−3.86 (m, 12), 4.10−4.20 (m, 2), 6.53−6.61 (m, 2), 6.89−7.15 (m, 2), 7.63 (s, 1H), 11.82 (s, exchangeable with D_2O, 1); MS (ESI$^+$) *m/z* 469 $(M + H)^+$. Anal. ($C_{26}H_{34}Cl_2N_2O_6$) C, H, N.

Biology. Functional Antagonism in Isolated Tissues. Male Wistar rats (275−300 g) were killed by cervical dislocation, and the organs required were isolated, freed from adhering connective tissue, and set up rapidly under a suitable resting tension in 20 mL organ baths containing physiological salt solution kept at 37 °C and aerated with 5% CO_2:95% O_2 at pH 7.4. Concentration−response curves were constructed by cumulative addition of agonist. The concentration of agonist in the organ bath was increased approximately 3-fold at each step, with each addition being made only after the response to the previous addition had attained a maximal level and remained steady. Contractions were recorded by means of a force displacement transducer connected to the MacLab system PowerLab/800. In addition, parallel experiments in which tissues did not receive any antagonist were run in order to check any variation in sensitivity.

Rat Vas Deferens Prostatic Portion. This tissue was used to assess α_{1A}-adrenergic antagonism.[21] Prostatic portions of 2 cm length were mounted under 0.5 g tension in Tyrode solution of the following composition (mM): NaCl, 130.0; KCl, 2.0; $CaCl_2$, 1.8; $MgCl_2$, 0.89; $NaHCO_3$, 25.0; NaH_2PO_4, 0.42; glucose, 5.6. Cocaine hydrochloride (0.1 μM) was added to the Tyrode to prevent the neuronal uptake of (−)-noradrenaline. The preparations were equilibrated for 60 min with washing every 15 min. After the equilibration period, tissues were primed two times by addition of 10 μM (−)-noradrenaline. After another washing and equilibration period of 60 min, a (−)-noradrenaline concentration−response curve was constructed (basal response). The antagonist was allowed to equilibrate with the tissue for 30 min, then a new concentration−response curve to the agonist was obtained. (−)-Noradrenaline solutions contained 0.05% $Na_2S_2O_5$ to prevent oxidation.

Rat Spleen. This tissue was used to assess α_{1B}-adrenergic antagonism.[23] The spleen was removed and bisected longitudinally into two strips that were suspended in tissue baths containing Krebs solution of the following composition (mM): NaCl, 120.0; KCl, 4.7; $CaCl_2$, 2.5; $MgSO_4$, 1.5; $NaHCO_3$, 20.0; KH_2PO_4, 1.2; glucose, 11.0; K_2EDTA, 0.01. (±)-Propranolol hydrochloride (4.0 μM) was added to block β-adrenoreceptors. The spleen strips were placed under 1 g resting tension and equilibrated for 2 h. The cumulative concentration−response curves to (−)-phenylephrine were measured isometrically and obtained at 30 min intervals, the first one being discarded and the second one was taken as control. The antagonist was allowed to equilibrate with the tissue for 30 min, then a new concentration−response curve to the agonist was constructed.

Rat Aorta. This tissue was used to assess α_{1D}-adrenergic antagonism.[22] Thoracic aorta was cleaned from extraneous connective tissue and placed in Krebs solution of the following composition (mM): NaCl, 118.4; KCl, 4.7; $CaCl_2$, 1.9; $MgSO_4$ 1.2; $NaHCO_3$, 25.0; NaH_2PO_4, 1.2; glucose, 11.7. Cocaine hydrochloride (0.1 μM) and (±)-propranolol hydrochloride (4.0 μM) were added to prevent the neuronal uptake of (−)-noradrenaline and to block β-ARs, respectively. Two helicoidal strips (15 mm × 3 mm) were cut from each aorta beginning from the end most proximal to the heart. The endothelium was removed by rubbing with filter paper: the absence of acetylcholine (100 μM)-induced relaxation to preparations contracted with (−)-noradrenaline (1 μM) was taken as an indicator that the vessel was denuded successfully. Vascular strips were then tied with surgical thread and suspended in a jacketed tissue bath containing Tyrode solution. Strips were secured at one end to Plexiglas hooks and connected to transducer for monitoring changes in isometric contraction. After at least a 2 h equilibration period under an optimal tension of 2 g, cumulative (−)-noradrenaline concentration−response curves were recorded at 1 h intervals, the first two being discarded and the third one taken as control. The antagonist was allowed to equilibrate with the tissue for 30 min before the generation of the fourth cumulative concentration−response curve to (−)-noradrenaline. (−)-Noradrenaline solutions contained 0.05% K_2EDTA and 0.9% NaCl to prevent oxidation.

Inhibition of AChE. The method of Ellman et al. was followed.[25] Five different concentrations of each compound were used in order to obtain inhibition of AChE activity comprised between 20 and 80%. The assay solution consisted of a 0.1 M phosphate buffer pH 8.0, with the addition of 340 μM 5,5′-dithiobis(2-nitrobenzoic acid), 0.035 unit/mL AChE derived from human erythrocytes (0.39 and 5.9 UI/mg, respectively; Sigma Chemical), and 550 μM acetylthiocholine iodide. Test compounds were added to the assay solution and preincubated at 37 °C with the enzyme for 20 min followed by the addition of substrate. Assays were done with a blank containing all components except AChE in order to account for nonenzymatic reaction. The reaction rates were compared and the percent inhibition due to the presence of test compounds was calculated. Each concentration was analyzed in triplicate, and IC_{50} values were determined graphically from log concentration−inhibition curves.

Radioligand Binding Assays. Binding to cloned human α_1-AR subtypes was performed in membranes from CHO (chinese hamster ovary) cells transfected by electroporation with DNA expressing the gene encoding each α_1-AR subtype. Cloning and stable expression of the human α_1-AR gene was performed as previously described.[24] CHO cell membranes (30 μg of proteins) were incubated in 50 mM Tris-HCl, pH 7.4, with 0.1−0.4 nM [^{3}H]prazosin, in a final volume of 1.02 mL for 30 min at 25 °C, in absence or presence of competing drugs (1 pM to 10 μM). Nonspecific binding was determined in the presence of 10 μM phentolamine. The incubation was stopped by addition of ice-cold Tris-HCl buffer and rapid filtration through 0.2% polyethyleneimine-pretreated Whatman GF/B or Schleicher & Schuell GF52 filters.

Molecular Modeling. Construction of the Models. Compound **1** was directly retrieved for the Cambridge Structural Database (CSD code YARTEQ) and its geometry was optimized at semiempirical Hamiltonian level AM1,[26] as implemented in the SYBYL (Tripos Inc. St. Louis, MO) graphic interface to MOPAC (keyword PRECISE). The molecular models of **2** and **3** were built by properly modifying the 7-methoxy-9-amino-1,2,3,4-tetrahydroacridine and 2,3-trimethylene-4-phenyl-6-chloropyridine skeletons retrieved from the CSD (CSD codes WIDDAO and TIBLEV, respectively) and by adding the proper fragments from the standard library of SYBYL. The models were minimized first by using steepest descent and then conjugate gradient until a convergence of 0.05 kcal mol^{-1} Å^{-1} on the gradient was reached. When needed, conformational searches were carried out, and the minimum energy conformers were further optimized by means of the AM1 method.

Conformational Search. The conformational analyses were carried out to sample the rotatable bonds of the furoyl substituent bound to the tricyclic skeleton. This was accomplished by means of Monte Carlo analyses[27] as implemented in MacroModel software.[28] In a Monte Carlo study, the phase space of a molecule is sampled by randomly changing dihedral angle rotations or atom positions. Then, the trial conformation is accepted if its energy has decreased from the previous one. If the energy is higher, various criteria can be applied to accept or reject the Monte Carlo trial. In the present simulations, the number of Monte Carlo steps was set equal to 8000 and the trial conformation was accepted if the energy was lower than that of the previous conformation or if its energy was within an energy window of 100 kJ/mol. Then, the conformations were classified by means of a cluster analysis[29] using geometrical parameters as filtering screens. The combined usage of Monte Carlo and cluster analyses has turned out to be a potent means for sampling the conformational space of highly flexible molecules.[30]

Data Analysis. In functional studies responses were expressed as percentage of the maximal contraction observed in the agonist concentration−response curve taken as a control. Pharmacological computer programs analyzed the agonist concentration−response curves. pK_B values of compounds **2**−**11** were calculated according to van Rossum.[31]

Binding data were analyzed using the nonlinear curve-fitting program Allfit.[32] Scatchard plots were linear in all preparations. All pseudo-Hill coefficients (nH) were not significantly different from unity ($p > 0.05$). Equilibrium inhibition constants (K_i) were derived from the Cheng−Prusoff equation,[33] $K_i = IC_{50}/(1 + L/K_d)$, where L and K_d are the concentration and the equilibrium dissociation constant of the radioligand. pK_i values are the mean ± SE of two or three separate experiments performed in triplicate.

Acknowledgment. Supported by grants from the University of Bologna and MIUR.

References

(1) Bylund, D. B.; Eikenberg, D. C.; Hieble, J. P.; Langer, S. Z.; Lefkowitz, R. J.; Minneman, K. P.; Molinoff, P. B.; Ruffolo, R. R., Jr.; Trendelenburg, U. International Union of Pharmacology nomenclature of adrenoceptors. *Pharmacol. Rev.* **1994**, *46*, 121−136.

(2) Hieble, J. P.; Bylund, D. B.; Clarke, D. E.; Eikenburg, D. C.; Langer, S. Z.; Lefkowitz, R. J.; Minneman, K. P.; Ruffolo, R. R., Jr. International Union of Pharmacology. X. Recommendation for nomenclature of α_1-adrenoceptors: Consensus update. *Pharmacol. Rev.* **1995**, *47*, 267−270.

(3) Daniels, D. V.; Gever, J. R.; Jasper, J. R.; Kava, M. S.; Lesnick, J. D.; Meloy, T. D.; Stepan, G.; Williams, T. J.; Clarke, D. E.; Chang, D. J.; Ford, A. P. Human cloned α_{1A}-adrenoceptor isoforms display α_{1L}-adrenoceptor pharmacology in functional studies. *Eur. J. Pharmacol.* **1999**, *370*, 337−343.

(4) Matyus, P.; Horvath, K. α-Adrenergic approach in the medical management of benign prostatic hyperplasia. *Med. Res. Rev.* **1997**, *17*, 523−535.

(5) Cooper, K. L.; McKiernan, J. M.; Kaplan, S. A. α-Adrenoceptor antagonists in the treatment of benign prostatic hyperplasia. *Drugs* **1999**, *57*, 9−17.

(6) Cavalli, A.; Lattion, A. L.; Hummler, E.; Nenniger, M.; Pedrazzini, T.; Aubert, J. F.; Michel, M. C.; Yang, M.; Lembo, G.; Vecchione, C.; Mostardini, M.; Schmidt, A.; Beermann, F.; Cotecchia, S. Decreased blood pressure response in mice deficient of the α_{1b}-adrenergic receptor. *Proc. Natl. Acad. Sci. U.S.A.* **1997**, *94*, 11589−11594.

(7) Giardinà, D.; Brasili, L.; Gregori, M.; Massi, M.; Picchio, M. T.; Quaglia, W.; Melchiorre, C. Structure−activity relationships in prazosin-related compounds. Effect of replacing a piperazine ring with an alkanediamine moiety on α_1-adrenoreceptor blocking activity. *J. Med. Chem.* **1989**, *32*, 50−55.

(8) Giardinà, D.; Gulini, U.; Massi, M.; Piloni, M. G.; Pompei, P.; Rafaiani, G.; Melchiorre, C. Structure−activity relationships in prazosin-related compounds. 2. Role of the piperazine ring on α-blocking activity. *J. Med. Chem.* **1993**, *36*, 690−698.

(9) Giardinà, D.; Crucianelli, M.; Melchiorre, C.; Taddei, C.; Testa, R. Receptor binding profile of cyclazosin, a new α_{1B}-adrenoceptor antagonist. *Eur. J. Pharmacol.* **1995**, *287*, 13−16.

(10) Giardinà, D.; Crucianelli, M.; Romanelli, R.; Leonardi, A.; Poggesi, E.; Melchiorre, C. Synthesis and biological profile of the enantiomers of [4-(4-amino-6,7-dimethoxyquinazolin-2-yl)-*cis*-octahydroquinoxalin-1-yl] furan-2-ylmethanone (cyclazosin), a potent competitive α_{1B}-adrenoceptor antagonist. *J. Med. Chem.* **1996**, *39*, 4602−4607.

(11) Bolognesi, M. L.; Budriesi, R.; Chiarini, A.; Poggesi, E.; Leonardi, A.; Melchiorre, C. Design, synthesis, and biological activity of prazosin-related antagonists. Role of the piperazine and furan units of prazosin on the selectivity for α_1-adrenoreceptor subtypes. *J. Med. Chem.* **1998**, *41*, 4844−4853.

(12) Minarini, A.; Budriesi, R.; Chiarini, A.; Leonardi, A.; Melchiorre, C. Search for α_1-adrenoceptor subtypes selective antagonists: Design, synthesis and biological activity of cystazosin, an α_{1D}-adrenoceptor antagonist. *Bioorg. Med. Chem. Lett.* **1998**, *8*, 1353−1358.

(13) Bolognesi, M. L.; Marucci, G.; Angeli, P.; Buccioni, M.; Minarini, A.; Rosini, M.; Tumiatti, V.; Melchiorre, C. Analogues of prazosin that bear a benextramine-related polyamine backbone exhibit different antagonism toward α_1-adrenoreceptor subtypes. *J. Med. Chem.* **2001**, *44*, 362−371.

(14) Campbell, S. F.; Davey, M. J.; Hardstone, J. D.; Lewis, B. N.; Palmer, M. J. 2,4-diamino-6,7-dimethoxyquinazolines. 1. 2-[4-(1,4-benzodioxan-2-ylcarbonyl)piperazin-1-yl] derivatives as α_1-adrenoceptor antagonists and antihypertensive agents. *J. Med. Chem.* **1987**, *30*, 49−57.

(15) Campbell, S. F.; Hardstone, J. D.; Palmer, M. J. 2,4-Diamino-6,7-dimethoxyquinoline derivatives as α_1-adrenoceptor antagonists and antihypertensive agents. *J. Med. Chem.* **1988**, *31*, 1031−1035.

(16) Bordner, J.; Campbell, S. F.; Palmer, M. J.; Tute, M. S. 1,3-Diamino-6,7-dimethoxyisoquinoline derivatives as potential α_1-adrenoceptor antagonists. *J. Med. Chem.* **1988**, *31*, 1036−1039.

(17) Ishiguro, M.; Futabayashi, Y.; Ohnuki, T.; Ahmed, M.; Muramatsu, I.; Nagatomo, T. Identification of binding sites of prazosin, tamsulosin and KMD-3213 with α_1-adrenergic receptor subtypes by molecular modeling. *Life Sci.* **2002**, *71*, 2531−2541.

(18) Melchiorre, C.; Angeli, P.; Bolognesi, M. L.; Chiarini, A.; Giardinà, D.; Gulini, U.; Leonardi, A.; Marucci, G.; Minarini, A.; Pigini, M.; Quaglia, W.; Rosini, M.; Tumiatti, V. α_1-Adrenoreceptor antagonists bearing a quinazoline or a benzodioxane moiety. *Pharm. Acta Helv.* **2000**, *74*, 181−190.

(19) Rosini, G.; Marotta, E.; Ballini, R.; Petrini, M. Coniugate addition of nitro-derivatives to α,β-unsaturated carbonyl compounds on basic allumina. *Synthesis* **1979**, *3*, 237−238.

(20) Nelson, W. L.; Powell, M. L.; Dyer, D. C. Absolute configuration of glycerol derivatives. 7. Enantiomers of 2-[[[2-(2,6-dimethoxyphenoxy)ethyl]amino]methyl]-1,4-benzodioxane (WB-4101), a potent competitive α-adrenergic antagonist. *J. Med. Chem.* **1979**, *22*, 1125−1127.

(21) Eltze, M.; Boer, R.; Sanders, K. H.; Kolassa, N. Vasodilatation elicited by 5-HT1A receptor agonists in constant-pressure-perfused rat kidney is mediated by blockade of α_{1A}-adrenoceptors. *Eur. J. Pharmacol.* **1991**, *202*, 33−44.

(22) Ko, F. N.; Guh, J. H.; Yu, S. M.; Hou, Y. S.; Wu, Y. C.; Teng, C. M. (−)-Discretamine, a selective α_{1D}-adrenoceptor antagonist, isolated from Fissistigma glaucescens. *Br. J. Pharmacol.* **1994**, *112*, 1174−1180.

(23) Buckner, S. A.; Oheim, K. W.; Morse, P. A.; Knepper, S. M.; Hancock, A. A. α_1-Adrenoceptor-induced contractility in rat aorta is mediated by the alpha 1D subtype. *Eur. J. Pharmacol.* **1996**, *297*, 241−248.

(24) Testa, R.; Taddei, C.; Poggesi, E.; Destefani, C.; Cotecchia, S.; Hieble, J. P.; Sulpizio, A. C.; Naselsky, D.; Bergsma, D.; Ellis, S.; Swift, A.; Ganguly, S.; Ruffolo, R. R., Jr.; Leonardi, A. Rec 15/2739 (SB 216469): A novel prostate selective α_1-adrenoceptor antagonist. *Pharmacol. Commun.* **1995**, *6*, 79−86.

(25) Ellman, G. L.; Courtney, K. D.; Andres, V.; Featherstone, R. M. A new rapid colorimetric determination of acetylcholinesterase activity. *Biochem. Pharmacol.* **1961**, *7*, 88−95.

(26) Dewar, M. J. S.; Zoebisch, E. G.; Healy, E. F.; Stewart, J. J. P. AM1: A new general purpose quantum mechanical molecular model. *J. Am. Chem. Soc.* **1985**, *107*, 3902−3909.

(27) Chang, G.; Guida, W. C.; Still, W. C. An internal coordinate Monte Carlo method for searching conformational space. *J. Am. Chem. Soc.* **1989**, *111*, 4379−4386.

(28) Mohamadi, F.; Richards, N. G. J.; Guida, W. C.; Liskamp, R. M. J.; Lipton, M. A.; Caulfield, C. E.; Chang, G.; Hendrickson, T. F.; Still, W. C. MacroModel−An integrated software system for modeling organic and bioorganic molecules using molecular mechanics. *J. Comput. Chem.* **1990**, *1*, 440−467.

(29) Shenkin, P. S.; McDonald, P. Q. Cluster analysis of molecular conformations. *J. Comput. Chem.* **1994**, *15*, 899−916.

(30) Cavalli, A.; Poluzzi, E.; De Ponti, F.; Recanatini, M. Toward a pharmacophore for drugs inducing the long QT syndrome: Insights from a CoMFA study of HERG K^+ channel blockers. *J. Med. Chem.* **2002**, *45*, 3844−3853.

(31) Van Rossum, J. M. Cumulative dose−response curves. II. Technique for the making of dose−response curves in isolated organs and the evaluation of drug parameters. *Arch. Int. Pharmacodyn. Ther.* **1963**, *143*, 299−330.

(32) DeLean, A.; Munson, P. J.; Rodbard, D. Simultaneous analysis of families of sigmoidal curves: Application to bioassay, radioligand assay, and physiological dose−response curves. *Am. J. Physiol.* **1978**, *235*, E97−102.

(33) Cheng, Y. C.; Prusoff, W. H. Relationship between the inhibition constant (K_i) and the concentration of inhibitor which causes 50% inhibition (I_{50}) of an enzymatic reaction. *Biochem. Pharmacol.* **1973**, *22*, 3099−3108.

JM030952Q